a comparison of model cross sections to those measured. Branching ratio tests determine that all excited levels of ^{35}Cl below 3.0 MeV decay by ground-state transitions with at most weak branches to other levels.

The comparisons in Table II show that the HF formalism provides cross sections within about 25% of measurements for levels of known spin, except that for the $\frac{7}{2}$ level at 2.645 MeV. The calculated angular distributions in Figs. 9–11 provide excellent fits to the measured distributions. In considering the success of this analysis, it is important to note that no parameters have been adjusted to improve fits to Cl$(n,n'\gamma)$ cross sections. Parameter adjustment stopped when the ^{39}K and ^{40}Ca data were successfully fitted. The effect of the neutron pair in ^{35}Cl would appear to be to lower the energies of positive parity levels more than 0.5 MeV. The negative-parity levels do not seem to be much affected. It would be interesting to know if one of the levels near 4-MeV excitation in ^{35}Cl corresponds to the 3.71-MeV level of ^{37}Cl.

ACKNOWLEDGMENTS

The authors are grateful for the generous cooperation of the University of Kentucky Computing Center and in particular to Selwyn Zerof for computational assistance. We acknowledge also the analytical assistance of J. L. Allison. The authors are also grateful to Dr. K. W. Jones, Brookhaven National Laboratory, who suggested to them the use of Ge(Li) detectors.

PHYSICAL REVIEW VOLUME 151, NUMBER 3 18 NOVEMBER 1966

Internal Conversion, Multipole Mixing, and Auger Spectrum in Zn^{67} from Ga^{67} Decay*

MELVIN S. FREEDMAN, FRED T. PORTER, AND FRANK WAGNER
Argonne National Laboratory, Argonne, Illinois
(Received 20 April 1966)

Absolute internal-conversion coefficients measured with high electron resolution and with a Ge(Li) spectrometer have been studied in seven transitions in Zn^{67} from 78-h Ga^{67} decay. From these and from L subshell ratios for the three lowest energy transitions, we deduce the following multipolarities: 93 keV, pure $E2$; 184 keV, $M1+(8$–$12\%\ E2)$; all others predominantly $M1$, with $E2$ required in the 91- and 494-keV transitions. The retardation factor of the l-allowed 91-keV transition is 500, which is larger than that (340) for the l-forbidden 184-keV transition ($E2$-component enhancement of 17) originating at the same level. Conversion data, together with a reanalysis of γ-γ angular-correlation measurements of Rietjens and Van den Bold, lead unambiguously to the following level spin assignments, in agreement with those from (d,p) stripping and Coulomb excitation: (keV, $J\pi$); ground state $\frac{5}{2}-$; 93.317 ± 0.02, $\frac{1}{2}-$; 184.595 ± 0.04, $\frac{3}{2}-$; 393.59 ± 0.04, $\frac{3}{2}-$; 887.87 ± 0.1, $\frac{3}{2}-$. Conversion coefficients show somewhat better agreement with those calculated by Sliv and Band (extrapolated from $Z=33$) than with those of Rose for the L shell, but indicate that both computations give L-shell coefficients too small ($\sim10\%$ for Sliv and Band, $\sim20\%$ for Rose) for this Z range. The empirical Z displacement rule for M_I conversion due to Chu and Perlman ($\Delta Z=-7.0$), which, applied to the unscreened, point-nucleus M conversion values of Rose gives agreement for all energies and multipolarities above $Z=50$, is found to require $\Delta Z=-9.5$ for agreement at $Z=30$. Six of nine predicted lines in the KLL Auger spectrum of Zn are resolved; energies determined are 7–13 eV above those calculated by Hörnfeldt, and intensities agree with recent experimental results at $Z=32$ except for the K-L_1L_3 ($^3P_1$) line, where our intensity is lower by a factor of 2.

I. INTRODUCTION

THE studies of Ketelle *et al.*[1] and of Meyerhof *et al.*[2] on the decay of 78-h Ga^{67} and of Easterday[3] on Cu^{67} produced an essentially complete and consistent level structure in Zn^{67}. (see Fig. 1). Of particular concern for the present studies are the spin assignments for the 93-keV, $T_{1/2}=9.3$ μsec metastable level and for the 184-keV level. Easterday[3] judged the 93-keV level to be $\frac{1}{2}-$, on the basis of the theoretical single-particle $E2$ half-life of 4.88 μsec; $M1$ mixing was ruled out since the $M1$ half-life is $\sim3\times10^{-11}$ sec. The conversion coefficient for the 93-keV transition obtained by Easterday, 0.5 ± 0.2, and by Ketelle *et al.*, 0.63, is consistent with pure $E2$, or within the error limits, with a 50% $M1$ admixture. In so far as $M1$ mixing is deemed to vanish in principle, the $\frac{1}{2}-$ assignment is supported. Meyerhof *et al.* tentatively suggested a $p_{3/2}$ character for the 93-keV level, and $\frac{5}{2}-$ for the 184-keV level. Easterday[3] and Ketelle *et al.*[1] assign $\frac{3}{2}-$ to the latter.

Gamma-gamma angular-correlation measurements

* Based on work performed under the auspices of the U. S. Atomic Energy Commission.
[1] B. H. Ketelle, A. H. Brosi, and F. M. Porter, Phys. Rev. **90**, 567 (1953).
[2] W. E. Meyerhof, L. G. Mann, and H. I. West, Jr., Phys. Rev. **92**, 758 (1953).
[3] H. T. Easterday, Phys. Rev. **91**, 653 (1953).

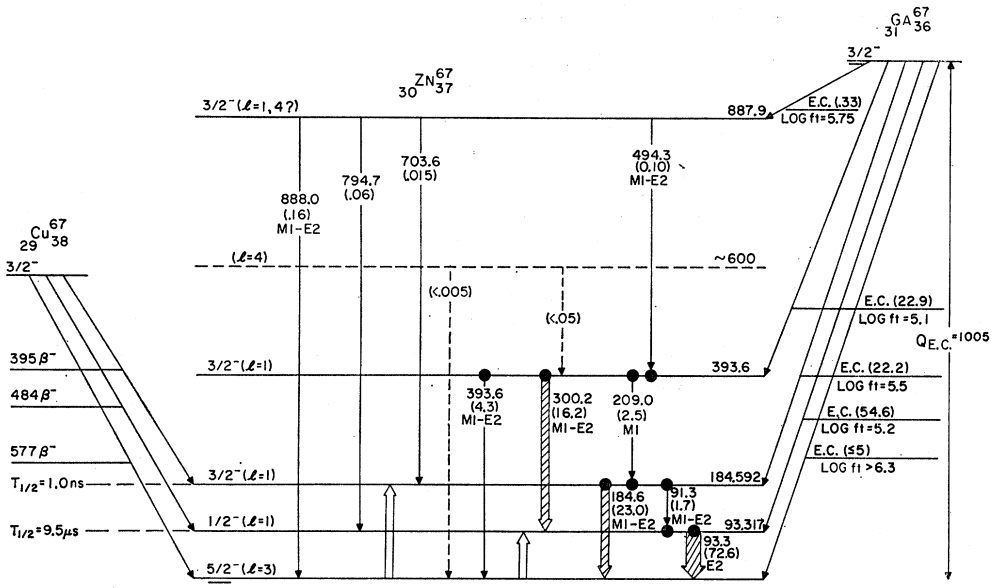

FIG. 1. Level scheme of Zn^{67} from this and previous work. In parentheses are intensities per decay of Ga^{67} in percent (assuming no capture to the ground state). l values from (d,p) stripping. Dots indicate coincidences.

of Rietjens and Van den Bold,[4] aimed at resolving these discrepancies appeared clearly to reject the $\frac{1}{2}$ spin for the 93-keV level and to agree with a $\frac{3}{2}$ spin, and for the 184-keV level to select $\frac{5}{2}$ over $\frac{3}{2}$ unambiguously. An analysis of these experiments is given in this paper showing that these conclusions erroneously stem from overly restrictive assumptions and that the correlations observed are consistent with the indicated spin sequences (Fig. 1) and with multipolarity admixtures in agreement with more precisely measured conversion coefficients.

Angular distributions of the 184- and (91+93)-keV gamma rays following Coulomb excitation by neon ions were studied by Ritter *et al.*,[5] and with nitrogen ions by Alkhazov *et al.*[6] The small direct excitation of the 93-keV level observed[5] is consistent with the level lifetime only if the 93-keV transition is pure $E2$, leading to a $\frac{1}{2}-$ assignment for the level. The angular distribution of the 184-keV gamma ray gave $\frac{3}{2}-$ for the level spin uniquely.[5,6] Both results were in disagreement with the conclusions of Rietjens and Van den Bold.[4]

Lin and Cohen[7] assigned $l=1$ and $l=3$ (tentatively) to the 93- and 184-keV levels, respectively, from angular distributions in the (d,p) stripping reaction on Zn^{66}. The $l=3$ assignment, which is subject to uncertainty because of the low stripping cross section and the intense 93-keV peak, agrees only with a $\frac{5}{2}-$ spin; the $l=1$ is, of course, consistent with either $\frac{1}{2}-$ or $\frac{3}{2}-$ for the 93-keV level.

Finally, in recent work at this laboratory[8] on angular distributions in (d,p) reactions on Zn^{66} between 20° and 160°, the sharp minimum at backward angles uniquely characterizing $J=\frac{1}{2}-$ final states[9] from even targets was seen for the 93-keV peak, but not for the 184-keV peak. Both peaks followed $l=1$ distributions over forward angles, yielding unique spins of $\frac{1}{2}-$ for the 93-keV and $\frac{3}{2}-$ for the 184-keV levels.

The strongest evidencd against these last assignments, with which all the beta- and gamma-ray spectroscopy either agree or are at least consistent, is the angular-correlation results of Rietjens and Van den Bold.[4] Their interpretation depends on the $M1$ purity of some transitions, based on the early crude conversion-coefficient measurements. Our motive was to refine these measurements at sufficiently good resolution to obtain multipolarity information from subshell ratios, as well as from absolute conversion coefficients, to resolve these ambiguities.

II. EXPERIMENTAL

A. Source Preparation

Very pure (<6 ppm impurity) natural-zinc foil was irradiated with 450 μA h of deuterons through an aluminum window which reduced the deuteron energy to 19 MeV. After three days of cooling to reduce the 9.5-h Ga^{66} activity, the foil was dissolved in concentrated HCl, ½ mg Ga carrier was added, and the gallium was extracted into 10% 2-ethyl hexanol in petroleum ether. After five scrubbings with 12 N HCl to remove zinc, the gallium was back extracted into distilled water. Gallium hydroxide was then pre-

[4] L. H. Th. Rietjens and H. J. Van den Bold, Physica **21**, 701 (1955).
[5] R. C. Ritter, P. H. Stelson, F. K. McGowan, and R. L. Robinson, Phys. Rev. **128**, 2320 (1962).
[6] D. G. Alkhazov, V. D. Vasil'ev, G. M. Gusinskii, I. K. Lemberg, and V. A. Nabichvrishvili, Izv. Akad. Nauk SSSR Ser. Fiz. **28**, 1683 (1964) [English transl.: Bull. Acad. Sci. Phys. Ser. **28**, 1575 (1964)].
[7] E. K. Lin and B. L. Cohen, Phys. Rev. **132**, 2632 (1963).
[8] J. P. Schiffer, D. Von Ehrenstein, and L. L. Lee, Jr., Bull. Am. Phys. Soc. **11**, 100 (1966).
[9] L. L. Lee, Jr., and J. P. Schiffer, Phys. Rev. **136**, B405 (1964).

cipitated with NH_4OH, but the yield in this step of the procedure was only about 20% by activity. Attempts to increase this yield by oxidation of the gallium with HNO_3, H_2O_2, and $KMnO_4$ or by carrying the activity on Fe $(OH)_3$ or additional gallium carrier were unsuccessful. This difficulty, not mentioned in the chemical literature,[4,10] persisted through three extraction procedures. The precipitation step was therefore avoided by simply reducing the volume of the HNO_3 acidified back-extract to $\sim 50\lambda$ and drying this on quartz wool.

In standard fashion, the wool was charged into the ion source in the Argonne electromagnetic isotope separator and gallium was volatilized in a stream of CCl_4 vapor. The mass-67 beam was decelerated at the target to 600 eV and deposited onto a 40-$\mu g/cm^2$ carbon film through a 1.5-mm diam hole in a covering mask plate. This invisible deposit served as source for the beta and gamma spectrometry for the low-energy transitions (≤ 300 keV). The source thickness was ~ 4 $\mu g/cm^2$, calculated from the impurity beam current at mass 67.

This impurity was seen on the oscilloscopic display of the beam current (to a fine wire mechanically swept through the ion beam) as a definite 5×10^{-9}-A peak at mass 67 and was definitely not a tailing from the Ga^{66} peak which was being collected simultaneously, nor was it Zn^{67} from zinc carried through the chemistry. Most probably it was a hydrocarbon ion. The Ga^{67} current was too small to be seen.

Higher energy electron and gamma spectroscopy was done on a 20 times more active $\frac{1}{4}$-in. diameter source on a 1-mil aluminum sheet, onto which the mass-67 beam was deposited at 50-keV ion energy.

B. Electron Spectrometry—Conversion-Line Intensities

The Argonne double-electron toroidal-field spectrometer[11] was used in the tandem mode focusing through both instruments in series. For the conversion lines of the 91-, 93-, and 184-keV transitions the electron trajectories were restricted to the angular range 60°–70° from the spectrometer axis giving a measured transmission (T) of 1.5% at 0.055% resolution (R; full width at half maximum, FWHM) with the 1.5-mm source. For the 209- and 300-keV lines the transmission zone was 40°–70° at $T=8.6\%$ and $R=0.10\%$. Higher energy lines were seen with the $\frac{1}{4}$-in. source at $T=12\%$ and $R=0.22\%$. The absolute spectrometer transmission was calibrated with a 1-mm Cs^{137} source standardized by 4π beta counting.

Figure 2 presents the conversion lines observed. Relative intensities of the lines observed in different modes were obtained by reference to the 93K or 184K lines which were surveyed in each mode. Decay corrections over a time spanning four half-lives were made using a 78-h half-life.[12] Table I gives the intensities per transition to excited states, i.e., per the sum of the 93-, 184-, 393-, and 888-keV transitions, each corrected for the

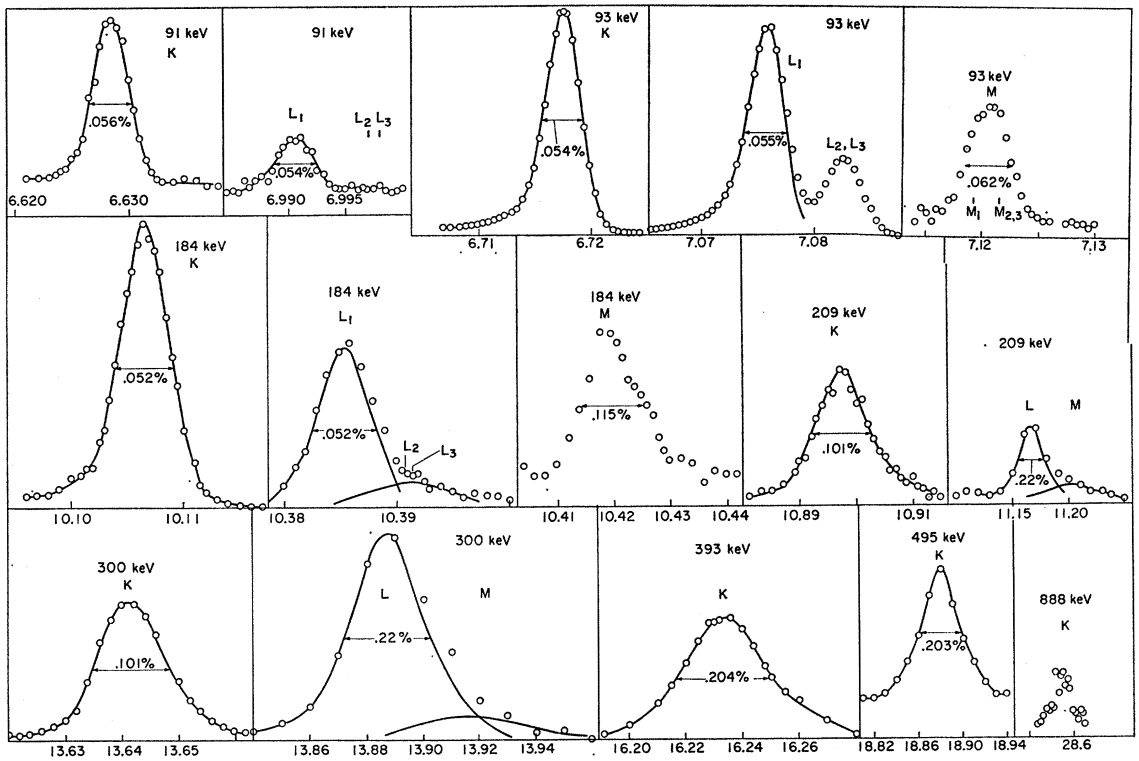

FIG. 2. Conversion lines from Ga^{67}, seen with various sources and resolutions.

[10] John E. Lewis, U. S. At. Energy Comm. NAS-NS 3032 (1961).
[11] M. S. Freedman, F. Wagner, F. T. Porter, J. Terandy, and P. P. Day, Nucl. Instr. Methods 8, 255 (1960); Bull. Am. Phys. Soc. 8, 526 (1963); and to be published.
[12] *Nuclear Data Sheets*, compiled by K. Way *et al.* (Printing and Publishing Office, National Academy of Sciences—National Research Council, Washington 25, D. C.), NRC 59-1-9.

observed conversion coefficients. This is equivalent to assuming that electron capture to the ground state is negligible; measurements[1,13] set a limit of 5% for this l-forbidden transition.

To account for the electrons in the line tails (6% for the 83-keV electron line), intensity comparisons were made using line areas integrated down to intersection of the tails with the background.

Table I also indicates an upper limit of 0.0004% per decay for the intensity of other conversion lines in the neighborhood of 200 keV obtained from a sweep over the range 182–298 keV. This search was made because the coincidence experiments of Rietjens and Van den Bold[4] gave indications of a gamma ray of ~200 keV with an intensity of ~0.1% per decay feeding the 393-keV level. A similar limit for the intensity of a 200-keV gamma ray was obtained from their gamma spectroscopy. A sweep over the range 568–640 keV gave an upper limit of 8×10^{-8}/decay for the conversion lines of ~600-keV gamma rays. (See discussion in regard to the 600-keV level.)

TABLE I. Internal-conversion lines from decay of Ga^{67}.

Transition (keV)	Conv. shell	Intensity per decay[a]
91	K	1.21±0.05(−3)
	L_1	1.25±0.10(−4)
	$L_{2,3}$	1.25±0.5(−5)
93	K	2.96±0.1(−1)
	L_1	2.72±0.25(−2)
	$L_{2,3}$	1.04±0.1(−2)
	M	5.1 ±0.5(−3)
184	K	3.55±0.1(−3)
	L_1	3.52±0.15(−4)
	$L_{2,3}$	3.5 ±0.7(−5)
	M	5.5 ±0.5(−5)
209	K	1.84±0.1(−4)
	L	1.75±0.15(−5)
300	K	5.4 ±0.2(−4)
	L	5.7 ±0.4(−5)
	M	7.3 ±1.0(−6)
393	K	8.2 ±0.5(−5)
494	K	1.20±0.05(−6)
888	K	5.2 ±1(−7)
568–640		≤8(−8)
182–298		≤4(−6)

[a] Number in parentheses is power of ten.

C. Gamma Spectrometry—Intensities

A 3.8-cm^2×5.5-mm thick lithium-drifted germanium detector and a 3 in.×3 in. NaI(Tl) scintillation spectrometer were used for the gamma-ray analysis, the latter specifically to obtain an additional value for the important 93-keV gamma-ray intensity. For this purpose the NaI crystal geometry was accurately established by x radiography of the potted crystal. The small correction for the absorption of the 93-keV gamma in the aluminum can and MgO reflector was evaluated from the measured intensity ratio[14] of the 2 -keV x ray in Ag^{109} to that of the 88.01-keV gamma ray. The source used was the same one used in the electron spectrometry. Using the efficiency curves of Heath,[15] one obtains the 93-keV gamma-ray intensity. This intensity, corrected for the 2.5% relative intensity of the 91-keV gamma unresolved in the peak, and averaged with the Ge (Li) detector intensity value, appears in Table II.

TABLE II. Gamma rays from decay of Ga^{67}.

Energy (keV)	Intensity per decay, including conversion electrons (%) This expt.	Rietjens[a] & Van den Bold	Ketelle *et al.*[b]	Meyerhof *et al.*[c]
91	$1.73_{-0.55}{}^{+0.25}$[d]	2.4	2.7	3.5
93	72.6 ±7	69	63.9	72.2
184	23.1 ±1.6	24	29.8	22.6
209	2.5 ±0.25	2.4	1	1.5
300	16.2 ±1.6	21.9	20.2	13.9
494	0.10 ±0.015	0.22	0.4	0.1
704	0.015±0.002	~0.1		0.05
795	0.06 ±0.01	0.1	0.2	0.1
888	0.16 ±0.016	0.2	0.4	0.3
~200	<0.05	0.1		
~600	<0.005	0.1		

[a] Reference 4. [b] Reference 1. [c] Reference 2. [d] Calculated assuming pure $M1$.

In the spectrum from the Ge(Li) detector (Fig. 3), one sees just the gamma rays deduced by Ketelle *et al.*[1] and by Meyerhof *et al.*[2] from the scintillation spectrum. The intensity of the 91-keV gamma ray is too small compared to the 93-keV gamma ray (~1:40) to be resolved. Separate runs expanding selected regions of the spectrum were examined for evidence of the 550–650 and ~200-keV gamma rays, leading to the upper intensity limits given in Table II.

A considerable effort has been made to determine the absolute and relative full-energy peak efficiency in two Ge(Li) detectors. Full description of these investigations is too lengthy for presentation here. We can summarize the somewhat disappointing results in the statement that the absolute efficiencies obtained from Ge detectors in this work have an uncertainty of 10–15% compared to estimates of 5–10% for NaI given by experienced workers.

For the efficiency measurement to be applied to the data of this experiment, samples of radioactivities with simple, well-known decay schemes were assayed, on a Ge(Li) and on a 3 in.×3 in. NaI detector. Figure 4

[13] A. Mukerji and P. Preiswerk, Helv. Phys. Acta **25**, 387 (1952).

[14] The ratio of K x rays to 88-keV gamma rays in Cd^{109} was measured by D. W. Engelkemeir of this laboratory to be 29.0±1.0, using NaI with beryllium windows. Wapstra and van der Eijk [Nucl. Phys. 4, 325 and 695 (1957)] obtained 23.8±0.7. Incidental to this determination we have measured the energy of the K conversion electrons and obtained a transition energy of 88.008±0.042 keV. Engelkemeir has measured the absorption coefficient in Pb and has found Pb K x rays from a lead backing on a Cd^{109} source. Both results prove the gamma energy exceeds the Pb K binding energy. This is given in Ref. 32 as 88.006 keV.

[15] R. L. Heath, U. S. Atomic Energy Commission Research and Development Report IDO-16880-1, 1964, 2nd ed., Appendix II (unpublished).

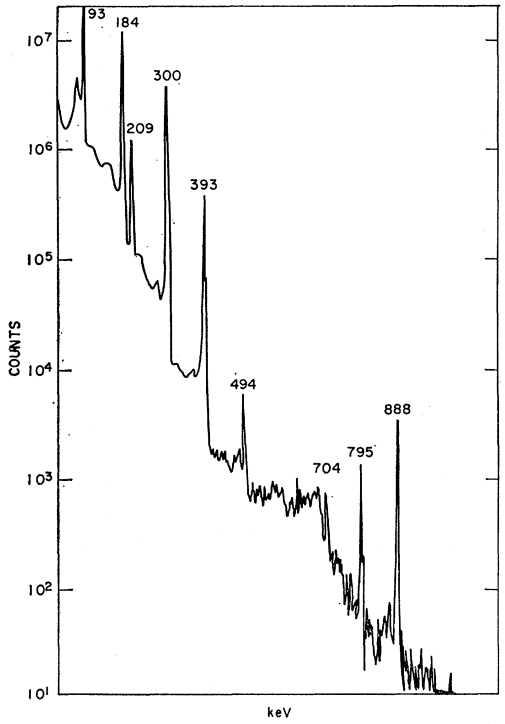

FIG. 3. Gamma-ray spectrum from Ga^{67}, on Ge(Li) detector.

shows the resulting efficiency curve for full-energy peaks, with experimental points. As is true in all cases we have examined, the curve is nearly linear on a log-log

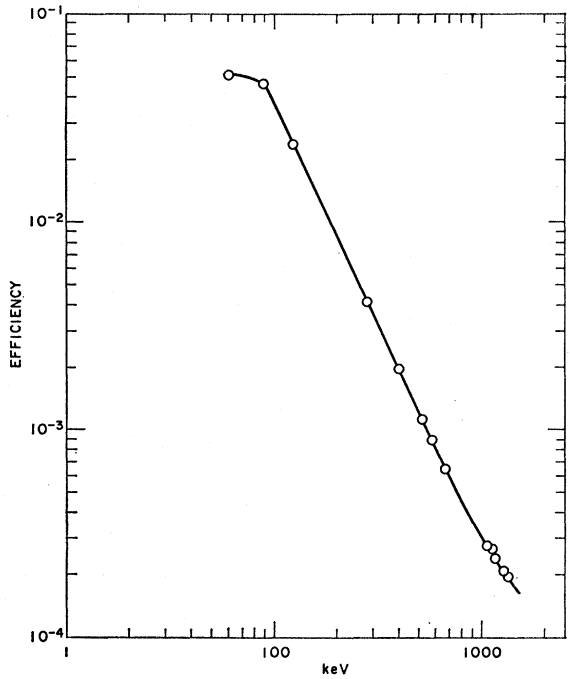

FIG. 4. Absolute efficiency of Ge(Li) detector (22-mm diam, 5.5-mm thick, sample 16.5 mm from detector face on axis) for full-energy peaks.

basis from 100 keV to over 1 MeV; usually it shows a reduced slope above 1–1.5 MeV.

Table II gives the absolute gamma-ray intensities per disintegration obtained in this work and from earlier studies. The value for the 93-keV gamma ray is the average of the Ge(Li) and NaI results, and the other gamma-ray intensities are adjusted to be in the ratios observed in Ge(Li) normalized to this average.

Only in the Cauchois bent-crystal-spectrometer measurements of Chupp, DuMond, Gordon, Jopson, and Mark[16] has the 91-keV gamma ray been clearly resolved. Professor Mark informs us that unfortunately the 93-keV line image is saturated on the plate, so no measurement of the relative intensity of the 91-keV transition is possible.

III. CONVERSION COEFFICIENTS

Table III presents the experimental and theoretical conversion coefficients and conversion ratios. Theoretical values are derived from Rose's[17] tables, and by an extrapolation of 3 units in Z, from Sliv and Band[18] (SB; lowest $Z=33$). This extrapolation was done graphically on a log α versus Z basis, on which the curves for K- and L_{I}-shell conversion coefficients are so nearly linear that the extrapolated values are valid to perhaps $\pm 1\%$. However, for some intermediate energies (200–300 keV) the L_{II}- and L_{III}-shell functions were so nonlinear over a range from $Z=33$–37 that the extrapolated values at $Z=30$ are uncertain to probably 20%.

In this Z region as well as in the higher Z range, as has recently been noted,[19,20] these two computations differ significantly (as much as 10–20%) in the L shells, and their ratio shows marked variation with energy and Z. Their agreement for the K shell is generally within 1%, and this is also true at $Z=30$, with the SB extrapolated values.

No definitive guides to a choice between the two sets of values exist. Although the SB values include contributions arising from dynamic or penetration effects, these amount, in normal cases, to only a few percent in the heavy elements and should be insignificant in this case. Moreover, practically all comparisons of experiment to these calculations are made in the medium- to heavy-element region where conversion coefficients are much higher and thus more easily measurable, and where subshell binding-energy differences are large enough to permit subshell conversion-electron resolution for reasonable transition energies.

---

[16] E. L. Chupp, J. W. M. DuMond, F. J. Gordon, R. C. Jopson, and H. Mark, Phys. Rev. **109**, 2036 (1958).

[17] M. E. Rose, *International Conversion Coefficients* (North-Holland Publishing Company, Amsterdam, 1958).

[18] L. A. Sliv and I. M. Band, *Alpha, Beta, and Gamma Spectroscopy* (North-Holland Publishing Company, Amsterdam, 1965), 2nd ed., Appendix 5.

[19] E. Seltzer and R. Hager, Phys. Letters **18**, 163 (1965); T. Novakov and J. M. Hollander, Nucl. Phys. **60**, 593 (1964).

[20] R. L. Graham, *Nuclear Spin-Parity Assignments* (Academic Press Inc., New York, 1966), p. 53.

TABLE III. Conversion coefficients and $M1$-$E2$ mixing in Zn^{67}.

Transition (keV)		K	$L_{I\text{ or tot}}$[b]	$K/L_{I\text{ or tot}}$[b]	K/M_{tot}	$L_I/(L_{II}+L_{III})$	Q,[a] derived from (%) K	$L_I/(L_{II}+L_{III})$	$K/L_{I\text{ or tot}}$[c]	$L_{I\text{ or tot}}$[c]
91	$\beta_1 S$[d]			11.1		26.4		0.8···4[e]	0[f]	
	$\alpha_2 S$			11.5		2.60				
	$\beta_1 R$[d]			12.8		17.3		0.2···3[e]	0[f]	
	$\alpha_2 R$			13.2		2.48				
	Expt.			9.7±1		10_{-3}^{+5}				
93	$\beta_1 S$	6.6(−2)[g]	5.9(−3)[g]	11.2		26.2	88···100[f]	100[e,f]	100···0[f]	96···100[f]
	$\alpha_2 S$	7.7(−1)	6.7(−2)	11.5		2.74				
	$\beta_1 R$	6.7(−2)	5.7(−3)	11.8	24	17.9	90···100[f]	85···53	0[f]	100[f]
	$\alpha_2 R$	7.6(−1)	5.7(−2)	13.3	19.4	2.49				
	Expt.	7.7±0.8(−1)	7.3±0.8(−2)	10.5±1	58±6	2.61±0.07				
184	$\beta_1 S$	1.13(−2)	9.9(−4)	11.4		28.4	8···12[e]	11···37	26···74	10···15
	$\alpha_2 S$	5.3(−2)	5.7(−3)	9.3		6.6				
	$\beta_1 R$	1.09(−2)	9.9(−4)	11.0	21	26.4	8···12	8···17	0[f]	14···22
	$\alpha_2 R$	5.8(−2)	5.1(−3)	13.1	20	5.0				
	Expt.	1.56±0.1(−2)	1.58±0.12(−3)	9.9±0.5	65±6	10±2				
209	$\beta_1 S$	8.3(−3)	7.6(−4)	10.9			0[f]		0[f]···17	0[f]···1.2
	$\alpha_2 S$	3.4(−2)	4.0(−3)	8.4						
	$\beta_1 R$	8.0(−3)	6.8(−4)	11.7	23.3		0[f]···0.7[e]		100[f]···1.6	0[f]···4.2
	$\alpha_2 R$	3.7(−2)	3.5(−3)	10.7	22.2					
	Expt.	7.5±0.7(−3)	7.1±1(−4)	10.6±1	61±20					
300	$\beta_1 S$	3.25(−3)	3.3(−4)	9.9			0[f]···7[e]		0[f]···97	0[f]···9
	$\alpha_2 S$	9.5(−3)	10.6(−4)	9.0						
	$\beta_1 R$	3.3(−3)	2.75(−4)	12.0	22.8		0[f]···6		100[f]	6···19
	$\alpha_2 R$	1.00(−2)	9.1(−4)	11.0	19.8					
	Expt.	3.37±0.3(−3)	3.5±0.3(−4)	9.5±0.5	75±10					
393	$\beta_1 S$	1.72(−3)					0[f]···16[e]			
	$\alpha_2 S$	3.85(−3)								
	$\beta_1 R$	1.75(−3)					1···15			
	$\alpha_2 R$	3.8(−3)								
	Expt.	1.92±0.15(−3)								
494	$\beta_1 S$	1.02(−3)					2···37			
	$\alpha_2 S$	1.89(−3)								
	$\beta_1 R$	1.05(−3)					0[f]···37[e]			
	$\alpha_2 R$	1.85(−3)								
	Expt.	1.19±0.15(−3)								
888	$\beta_1 S$	2.9(−4)					0[f]···100[e,f]			
	$\alpha_2 S$	3.55(−4)								
	$\beta_1 R$	2.95(−4)					0[f]···100[f]			
	$\alpha_2 R$	3.7(−4)								
	Expt.	3.37±0.7(−4)								

[a] $Q=E2/(M1+E2)$. The Q values given are calculated assuming only $E2$ and $M1$ contributions, i.e., no $E0$ or $M3$.
[b] Value is L_I if $L_I/(L_{II}+L_{III})$ value is given for the transition; if not, value is L_{tot}.
[c] Q values not used because of indications of incorrect L-shell theoretical calculations (see text).
[d] S=Sliv and Band (Ref. 18); R=Rose (Ref. 17).
[e] Accepted value or range of Q.
[f] Q value derived is negative or above 100%, i.e., experimental limit falls outside theoretical $M1$-$E2$ range.
[g] Number in parentheses is power of ten.

We therefore present both Rose's and SB's values for $Z=30$, for comparison to experiment. In columns 8 to 11 of Table III are given the multipole mixings derived from the relative and absolute conversion coefficients. In spite of the experimental errors and the uncertainties of extrapolation of SB's calculations to $Z=30$, there is some indication in the five lowest energy transitions of a significantly better internal consistency of the $E2$-$M1$ mixing fraction from different shells using SB's data than using Rose's. Our data indicate that both calculations of L-conversion coefficients are low by 10–20% for $M1$ and $E2$ transitions at $Z=30$.

In four cases, the 93-, 184-, 209-, and 300-keV transitions, M-conversion electrons were resolved (Fig. 2 and Table III). The ratios of their intensities to those of the K-conversion electrons are between 3 and 4 times smaller than Rose's values for $Z=30$, the only available calculations. These were computed on the basis of point nuclear charge with no correction for the important effects of electron screening. Various efforts to derive the screening effect on M conversion are underway.[21]

[21] R. F. O'Connell and C. O. Carroll, International Conference on the Internal Conversion Process, Vanderbilt University, 1965, (unpublished), Contribution 31, and C. P. Bhalla, *ibid.*, Contribution 34.

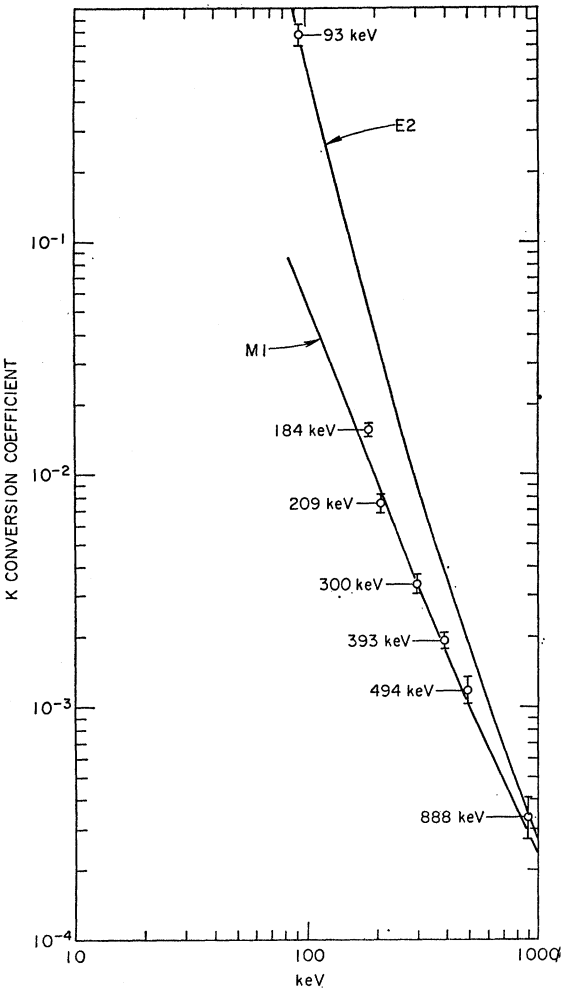

FIG. 5. K conversion coefficients in Zn^{67}.

Chu and Perlman[22] have shown that, for any multipolarity and energy, and for a wide range of Z ($Z \geq 50$), a set of empirical "screening" correction constants gives good agreement for M-subshell conversion. Conversion coefficients are obtained from Rose's tables at a value of $Z_{\text{effective}}$ given by $Z_{\text{eff}}=Z-\sigma_i$, where $\sigma_i=7.0$ for M_{I}, 7.9 for $M_{\text{II,III}}$, or 10.0 for $M_{\text{IV,V}}$. We can here explore the extension of this agreement to $Z=30$, which requires an extrapolation of Rose's M-shell (total) conversion coefficients to $Z=Z_{\text{eff}}\approx 20$. In this graphical extrapolation, two values in Rose's tables, at $k=0.6$, $Z=25$, and $Z=30$, appear to be in error, as they lie far from smooth curve values.

In Table IV we show the range of σ_{eff} ($=Z-Z_{\text{eff}}$) values obtained from the extrapolation, which gives agreement for four cases with the experimental error limits on total M conversion. For the 184- and 300-keV transitions, we include the effect of the experimentally allowed range of Q, the $E2$ mixing fraction.[23] We conclude that for $Z=30$ and $M1$-$E2$ transitions, that $\sigma_{\text{eff}}\sim 9.5\pm 0.6$. For such transitions, M_{I}-subshell conversion should dominate; a rough guide should be furnished by $M_{\text{I}}/(M_{\text{II}}+M_{\text{III}})\approx L_{\text{I}}/(L_{\text{II}}+L_{\text{III}})\approx 2.5-10$ (see Table III), with an $(M_{\text{IV}}+M_{\text{V}}+N)$ contribution no more than a few percent to total M conversion. From the shape of the unresolved composite M line of the 93-keV $E2$ transition (see Fig. 2), the ratio $M_{\text{I}}/(M_{\text{II}}+M_{\text{III}})$ may be about 1, rather than as large as expected. Thus a value between Chu and Perlman's value $\sigma_{M_{\text{I}}}=7.0$ and $\sigma_{M_{\text{II,III}}}=7.9$ would be predicted for $\sigma_{M,\text{total}}(\equiv\sigma_{\text{eff}})$; our value of 9.5 ± 0.6 indicates a significant Z dependence of the σ_i.[24]

TABLE IV. M-shell conversion coefficients and values of $\sigma_{\text{eff}}=Z-Z_{\text{eff}}$.

Transition (keV)	Q (%)	α_M(Expt.)[a,b]	Z_{eff}[c]	σ_{eff}[c]
93	100	$1.32\pm 0.18(-2)$	19.5 ± 1	10.5 ± 1
209	0	$1.23\pm 0.3(-4)$	$22\ \pm 2$	$8\ \pm 2$
184	10 ± 2	$2.4\ \pm 0.3(-4)$	$21\ \pm 1$	$9\ \pm 1$
300	3 ± 0.3	$4.5\ \pm 0.7(-5)$	20.8 ± 0.8	9.2 ± 0.8
			Weighted av.	9.5 ± 0.6

[a] From α_K and K/M, Table III.
[b] Numbers in parentheses are powers of ten.
[c] Errors in Z_{eff} and σ_{eff} propagated from α_M and $E2$-$M1$ mixing uncertainties.

Figure 5 presents the K-conversion coefficients for all transitions except the 91 keV. As from Table III one sees the $E2$ character of the 93-keV transition, the $M1$ dominance of the others and the experimental indeterminacy of the 888-keV mixing.

IV. LEVEL SPINS AND PARITIES

We return to the questions discussed in the Introduction. We first indicate the evidence favoring the assignments of Fig. 1 and then present Rietjens and Van den Bold's[4] arguments and a reanalysis of their results.

Ground state. The ground-state spin of Zn^{67} has been measured as $\frac{5}{2}$. Possible configurations involving the 37th neutron are $(f_{5/2})^3{}_{5/2}$ or $(f_{5/2})^5{}_{5/2}$. Shell-model arguments are fairly strong for negative parity for all levels up to several hundred kilo-electron volts. The ground-state spin of Ga^{67} has also been measured as $\frac{3}{2}$, consistent with shell-model predictions for the 31st

[22] Y. Y. Chu and M. L. Perlman, Phys. Rev. 135, B319 (1964).
[23] $Q\equiv E2/(E2+M1)=\delta^2/(1+\delta^2)$; $\delta^2\equiv E2/M1$.

[24] *Note added in proof.* Recent calculations of internal-conversion coefficients (ICC) for K, L, and M subshells have been made by C. P. Bhalla (private communication), at $Z=30$ and at our transition energies. These were based both on a "no-penetration" model (Rose's) and a surface-current model (Sliv and Band) with finite-size effects included, but with a self-consistent fully relativistic treatment of screening. The ICC with either model agree within $<1\%$ for all shells and show: (1) All L subshells increase by 10–20% with respect to the previous tabulations (Thomas-Fermi-Dirac screening model) to now give good agreement with our experimental results in all cases [Q values from L-ICC are now consistent with those from K shell and $L_{\text{I}}/(L_{\text{II}}+L_{\text{III}})$ as given in Table III]; (2) M-shell ICC now agree with experimental results in all cases (no effective Z displacement required).

proton, $p_{3/2}$. A fairly high lower limit,[1] $\log ft \geq 6.3$, for electron capture to the ground state, can arise from the l forbiddenness of the $(J\pi)$ allowed transition. Deuteron stripping[7,8] shows $l=3$.

93-keV level. The 93-keV level spin is almost certainly $\frac{1}{2}-$ from the strong evidence of the (d,p) angular distributions,[8] the $B(E2)$ obtained from direct Coulomb excitation,[5,6] and the measured lifetime of the state.[3,12] Our measurements (Table III) for K and $L_I/(L_{II}+L_{III})$ conversion coefficients of the 93-keV transition all are consistent with pure $E2$ values of Sliv and Band, and of Rose [with the exception of Rose's $L_I/(L_{II}+L_{III})$ ratio, where a 2% change will bring agreement]. Allowed electron capture (EC) to this state ($\log ft=5.2$ if no EC to ground) is consistent with this spin. The measured half-life of the level, 9.3 μsec,[12] corrected for the total conversion coefficient of 0.89, gives an $E2$ gamma-ray half-life of 17.6 μsec. The retardation factor with respect to the Weisskopf pure $E2$ estimate, 4.88 μsec, is 3.6, indicating the 93-keV state is a good single-particle $p_{1/2}$ state.

184-keV level. Angular distributions of the 184-keV gamma rays following Coulomb excitation[5,6] unambiguously lead to a $\frac{3}{2}-$ spin for the 184-keV level, as does the (d,p) angular distribution.[8] $M1$ mixing in the 184-keV transition is certain (8–12% $E2$, Table III) which limits the possibilities to $\frac{3}{2}-$, $\frac{5}{2}-$, or $\frac{7}{2}-$. $M1$ mixing in the 91-keV transition (96–100%), together with $\frac{1}{2}-$ for the 93-keV level selects $\frac{3}{2}-$. $\log ft=5.5$ is consistent with this choice. The uncertain value $l=3$ from[7] (d,p) is in disagreement. From the range in Q determined from the K conversion coefficient of the 184-keV transition, 0.08–0.12, the range of the amplitude mixing factor $|\delta| = |\langle E2\rangle/\langle M1\rangle|$ is 0.29–0.37. This does not overlap with the value $\delta=+0.51\pm0.07$ obtained by Ritter *et al.*,[5] but it does agree with $\delta=+0.345\rightarrow0.49$ from the similar angular distribution following Coulomb-excitation studies of Alkhazov *et al.*[6] From the weighted average (our and Ref. 6) $\delta=0.35\pm0.035$, the $(1.45\pm0.15)\times10^{-9}$ sec mean life[25] of the level and the 184-keV branching ratio from the level of 0.93 ± 0.03, we calculate a value of $\epsilon B(E2)=0.036\pm0.007$. Ritter *et al.*[5] obtained $\epsilon B(E2)=0.018\pm0.003$, while Temmer and Heydenburg[26] found 0.032, in better agreement. Ritter's $\epsilon B(E2)$ and δ value correspond to a level mean lifetime of 2.2×10^{-9} sec, 50% too large.

For the 91-keV transition, Ritter *et al.*[5] obtained a value of $|\delta| \leq 0.07$, from the observed angular distribution of the gamma ray in Coulomb excitation. This indicates even less $E2$ component than the limit from our $L_I/(L_{II}+L_{III})$ ratio, $|\delta| \leq 0.2$.

The 91- and 184-keV transitions are interesting as a pair of (mainly) $M1$ transitions originating from the same level, with the latter being l forbidden and the former l allowed. The 91-keV transition was (erroneously) included in the survey of Govil and Khurana[27] as an l-forbidden $M1$ transition, according to the former level spin assignments, $(\frac{5}{2}-) \rightarrow (\frac{3}{2}-)$. The experimental $M1$ matrix element therein calculated should be reduced by $\frac{2}{3}$ owing to the change in initial spin. As it was previously about tenfold below the values for other neighboring cases, the discrepancy is increased. This indicates that it is one of the rather retarded *l-allowed* $M1$ transitions recently noted by Murthy *et al.*[28] In fact, the retardation factors relative to single-particle Weisskopf estimates for the transitions are: 340 for the 184-keV $M1$ component and 500 for the 91-keV $M1$, i.e., larger for the l-allowed than for the l-forbidden transition, similar to three cases listed by Murthy *et al.*, Cd^{118}, Sb^{121}, and Au^{198}. For the $E2$ component of the 184-keV gamma, (assumed 10%, see Table III), the enhancement factor is 17 relative to the Weisskopf $E2$ rate.

393-keV level. The conversion coefficients require the 300-, 393-, and 209-keV transitions to be mainly $M1$ (the latter one perhaps pure $M1$). The only spin assignment for the 393-keV level consistent with $\frac{5}{2}-$ for the ground state and $\frac{1}{2}-$ for the 93-keV level is then $\frac{3}{2}-$. $M1$ for the 209-keV transitions and $\log ft=5.1$ are in agreement, as is the $l=1$ assignment from (d,p) stripping.[7,8]

888-keV level. The K-conversion coefficient of the 494-keV gamma ray clearly shows a strong $M1$ component which restricts the level spin choices to $\frac{1}{2}-$, $\frac{3}{2}-$, or $\frac{5}{2}-$. Allowed electron capture ($\log ft=5.75$) to this level imposes the same constraints. All four transitions which de-excite this level are of (roughly) comparable reduced transition probability. Were any of the transitions pure $E2$, it would have to be enhanced over the single-particle $E2$ rate by the order of one-thousandfold with respect to the other, $M1$ mixed, transitions (particularly the 494-keV) to be observed. A level spin of $\frac{1}{2}-$ $(\frac{5}{2}-)$ would make the 888 (795)-keV gamma ray pure $E2$. Unfortunately the theoretical $M1$ and $E2$ conversion coefficients are only 20% apart at 888 keV, too close to give positive experimental verification of an $M1$ component in the 888-keV gamma ray. Although the central experimental value lies in the range of $M1$-$E2$ mixing, the error band encompasses the entire range. From the relative lifetime arguments, the indication is for a spin of $\frac{3}{2}-$. Lin and Cohen,[7] by (d,p) stripping with 15-MeV deuterons and 90-keV resolution, excited the state weakly (0.2 mb); from angular distributions they proposed a double assignment, $l=1$ and $l=4$ to the level. The latter is inconsistent with the all decay data (gamma rays, $\log ft$, angular correlation of 494–300-keV gamma rays); the former value is consistent. The level is not visibly excited with 10-MeV deuterons.[29]

---

[25] R. E. Holland and F. J. Lynch, Phys. Rev. **121**, 1464 (1961).
[26] G. M. Temmer and N. P. Heydenburg, Phys. Rev. **104**, 967 (1956).
[27] I. M. Govil and C. S. Khurana, Nucl. Phys. **60**, 666 (1964).
[28] A. S. Venkatesha Murthy, S. M. Brahman, and M. K. Ramaswamy, Nucl. Phys. **67**, 369 (1965).
[29] D. von Ehrenstein and J. P. Schiffer (private communication).

600-keV level. Both Lin and Cohen[7] and Schiffer *et al.*[8] agree on $l=4$ for this state from (d,p) stripping. Probably this is the lowest $g_{9/2}$ intrinsic neutron excitation. Electron-capture decay to $l=4$ is either first forbidden unique or (likely) third forbidden; neither case would lead to observable intensities of the de-exciting transitions. Yet Rietjens and Van den Bold[4] found a gamma ray of ~200 keV in coincidence with the 300- and 393-keV gamma rays, of intensity 0.1% per decay, which they allocate between the ~595 and 393-keV levels. Decomposition of their NaI singles spectrum yielded a (ground-state-feeding) gamma ray of 595 keV, (0.1% per decay). From our Ge(Li) and conversion-electron measurements we can set conservative upper limits on the intensities of these gamma rays of 0.05% (~200 keV) and 0.005% (~600 keV) per decay, in agreement with expectations based on the $l=4$ assignment. However, Rietjens' results remain an unexplained ambiguity in the over-all picture.

V. GAMMA-GAMMA ANGULAR CORRELATIONS

Rietjens and Van den Bold[4] measured the angular correlations of the 209–184-keV and the 496–300-keV γ–γ cascades. For the former, with the assumption based on early conversion coefficient measurements that both transitions were *pure* $M1$, they showed that the only spin sequence fitting the observed correlation (anisotropy $=-0.216\pm0.008$) is $\frac{3}{2}-\frac{5}{2}-\frac{5}{2}$; thus the 184-keV level was assigned $\frac{5}{2}-$. Then, (from anisotropy $=+0.27\pm0.05$) for the 494–300-keV angular correlation with the assumption that the 300-keV transition is *pure* $M1$, but allowing up to a few percent $E2$ admixture in the 494-keV gamma, the possible spin sequences were reduced to: (a) $\frac{1}{2}-\frac{3}{2}-\frac{1}{2}$; (b) $\frac{5}{2}-\frac{3}{2}-\frac{1}{2}$; and (c) $\frac{3}{2}-\frac{3}{2}-\frac{3}{2}$. Several other possibilities, in which the angular-correlation analysis required at least 18% $E2$ component in the 494-keV transition were rejected as demanding too large a "slowing down" factor (≥ 500) to keep this transition competitive to the other three branches from the 888-keV level. Sequences (a) and (b), together with $\frac{5}{2}-$ for the 184-keV level, would make the 91-keV gamma ray pure $E2$; as this was unacceptable (conversion coefficient, partial lifetime of gamma rays), sequence (c) was chosen, and the 93-keV level was assigned $\frac{3}{2}-$.

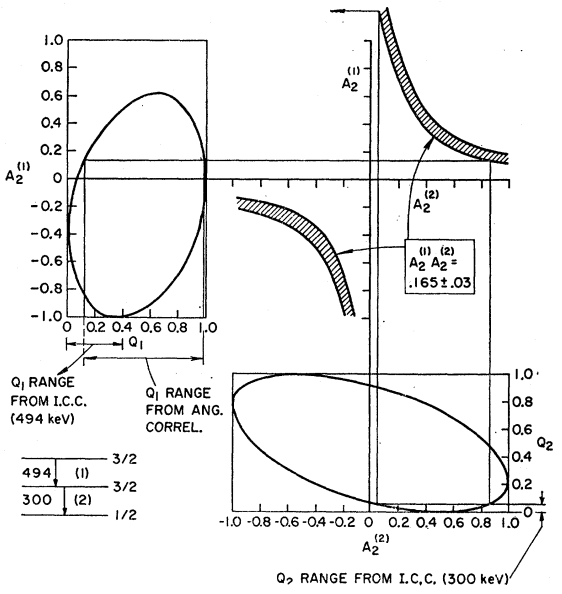

FIG. 6. Analysis of 494–300-kev γ-γ angular-correlation experiment of Ref. 4, with $E2$-$M1$ mixing in *both* transitions. Assumed spin sequence is that of Fig. 1. $W(\theta)=1+A_2^{(1)}A_2^{(2)}P_2(\cos\theta)$; $A_2^{(1)}A_2^{(2)}=0.165\pm0.03$ determines the hyperbolic error band. The range of Q_2, the quadrupole mixing fraction in the 300-keV transition, from conversion coefficients, 0–7%, determines a range of Q_1 of 12–98%; from ICC, $Q_1=0$–37%.

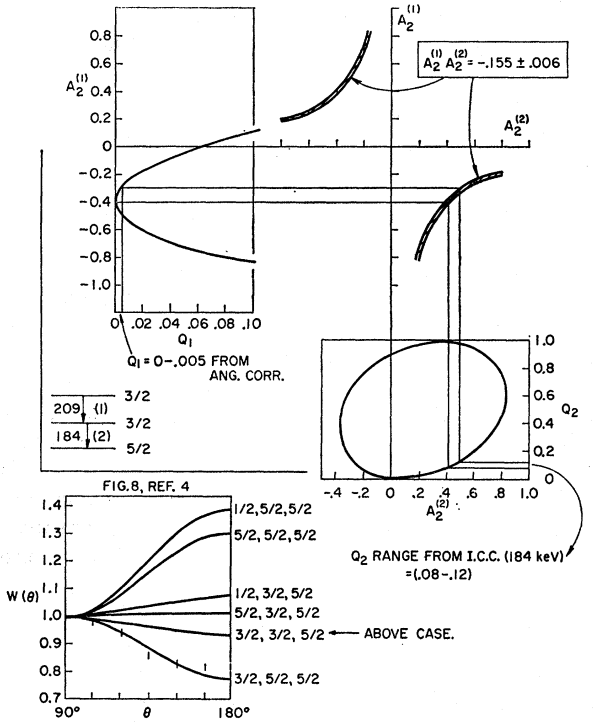

FIG. 7. Analysis of the 209–184-keV γ-γ angular correlation experiment of Ref. 4 with $E2$-$M1$ mixing in both transitions. Upper section is for assumed spin sequence $\frac{3}{2}$-$\frac{3}{2}$-$\frac{5}{2}$. $A_2=A_2^{(1)}A_2^{(2)}=-0.155\pm0.006$, from results of Ref. 4, determines hyperbolas. The range of Q_2 (184-keV quadrupole fraction) from internal conversion, 0.08–0.12, limits the range of Q_1 to 0–0.005; from conversion, $Q_1\leq0.007$. Lower part is Fig. 8 of Ref. 4; curves are theoretical, for indicated spin sequences, for both transitions as *pure* $M1$. Arrow shows spin sequence of upper part of figure.

Figure 6 shows our reanalysis of the 494–300-keV angular correlation results of Rietjens, but allowing both transitions to be $M1$-$E2$ mixtures. The spin sequence chosen is $\frac{3}{2}-\frac{3}{2}-\frac{1}{2}$ (Fig. 1) and the method is that of Arns and Wiedenbeck.[30] Rietjens and Van den Bold's[4] measured anisotropy of 0.27 ± 0.05 yields

[30] R. G. Arns and M. L. Wiedenbeck, Phys. Rev. **111**, 1631 (1958).

$A_2=A_2^{(1)}A_2^{(2)}=0.165\pm0.03$ as the coefficient of $P_2(\cos\theta)$. The upper limit of $E2$ admixture in the 300-keV γ ($Q_2=7\%$) from our conversion coefficients (Table III), combined with the measured anisotropy restricts Q_1(494 keV) to the range (12–98%), with ample overlap to the range (0–37%) for Q_1 determined from K conversion. This spin sequence is therefore consistent with all data. Although the "slowing down" factor compared to a pure $M1$ single-particle transition, for the 494-keV gamma ray is then at least 185 (i.e., $Q_1\geq12\%$), this is not unacceptable in view of the unknown mixings in the other three transitions from the 888-keV lever.

A similar analysis for the 209–184 keV gamma-ray cascade, for our spin sequence $\frac{3}{2}-\frac{3}{2}-\frac{5}{2}$ (Fig. 1), with $M1$-$E2$ mixing permitted for both transitions (in fact, demanded for the 184-keV gamma ray by our data) is shown in Fig. 7. The measured[4] anisotropy, -0.216 ± 0.008, gives $A_2^{(1)}A_2^{(2)}=-0.155\pm0.006$. Here the range on Q_2 (184 keV) from our conversion coefficients, 8–12%, together with Rietjens anisotropy, limits Q_1 (209-keV) to the range 0–0.4%, in agreement with the very small $E2$ admixture indiated by the conversion coefficients ($Q_1\leq0.7\%$). On the other hand, pure $M1$ for the 184-keV gamma ray as assumed by Rietjens and Van den Bold is not consistent with this spin sequence and the angular-correlation results. Again our spin sequence satisfies all the data. In the lower part of Fig. 6 is a copy of Fig. 8 of Ref. 4 in which the angular correlation for the 209–184 keV gamma-ray cascade is shown, together with various theoretical correlations, assuming both transitions are *pure* $M1$. This choice obviously rejects our $\frac{3}{2}-\frac{3}{2}-\frac{5}{2}$ spin sequence, yet allowing the indicated relatively small $E2$ admixture drastically alters this distinction.

VI. TRANSITION ENERGIES

We can obtain rather precise energy determinations for most transitions in Zn^{67} because of the good resolution realized for many of the conversion electrons. The problem of calibration of the beta spectrometer gives rise to the largest error components in such measurements.

We used the method of Siegbahn and Edvarson,[31] in which the momentum ratio between two electrons from the same transition, but converted in different shells, is combined with the known shell binding-energy difference to deduce the electron momenta. This was applied to the 91-, 93-, and 184-keV K and L_I conversion electron pairs.

Figure 8 shows these calibration values plus that from a Cs^{137} separately mounted standard source (error mainly due to uncertainty in Cs^{137} gamma-ray energy). It also illustrates the shift in calibration constant due to relative axial displacement of the source with respect to the standard and the error arising from a $1:10^5$ shift in the momentum ratio of the K-L_I pairs at 93- and 184-keV. The sensitivity due to a 1-eV shift in the K-L_I binding energy difference for $Z=30$ is also shown. Binding energies were taken from Hagstrom *et al.*[32]; $K=9.659$ and $L_I=1.196$ keV. These have been subject to reductions of 3 and 4 eV, respectively, in the last dozen years. An indication of the accuracy of L_I binding energies in this region is a recent redetermination[33] of the value for Kr ($Z=36$), which resulted in a 1-eV increase. Thus a 1-eV uncertainty in the binding-energy difference for $Z=30$ was folded ito the total error.[34]

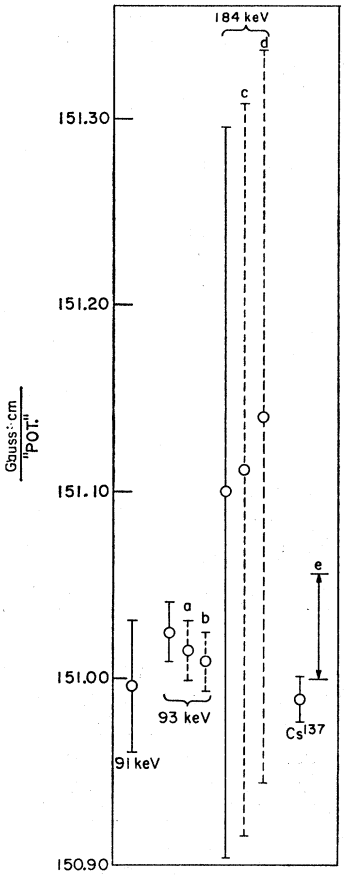

FIG. 8. Calibration constants of toroidal beta spectrometer from various calibration methods. Solid error bars labeled 91, 93, and 184 keV are derived from K, L_I conversion line pairs for each of these transitions, and the K-L_I electron-shell binding-energy difference. Dashed lines a and c show the effect of a 1-eV change in this binding-energy difference, and b and d the effect of $1:10^5$ change in the measured K/L_I momentum ratio. The bar Cs^{137} is the constant from a separate Cs^{137} standard source, and the arrow e shows the shift in calibration constant with 0.005 in. axial displacement of the source (uncertainty in position of edge-supported source film).

It was found that the crossover-stopover energy difference is much less sensitive to variation of the calibration constant than is the K-L_I binding-energy comparison. This can also be deduced from the equations of Bartlett.[35] From the data of Table V, the energy match 184- (91+93)-keV is 3 eV, compared to a combined error of 50 eV for the comparison.

We use the so-called "top-peak-center" definition of

[31] K. Siegbahn and K. Edvarson, Nucl. Phys. **1**, 137 (1956).

[32] S. Hagstrom, C. Nordling, and K. Siegbahn, *Alpha, Beta, and Gamma Spectroscopy* (North-Holland Publishing Company, Amsterdam 1965), 2nd ed., Appendix 2.

[33] M. O. Krause, Phys. Rev. **140A**, 1845 (1965).

[34] The following items and their contributions to the uncertainties were considered: imperfections in the compensation of the external magnetic field, $<1:10^6$; current control stability, $<3:10^6$; current control reference resistor, temperature effects, $<5:10^7$; voltage dividers, $1:10^5$; temperature effects on spectrometer dimensions, $<1:10^5$. All these contributions were neglected.

[35] A. A. Bartlett, Nucl. Instr. Methods **34**, 181 (1965).

TABLE V. Transition energies (keV).

Conversion line	E_γ[a]	$E_{\gamma(\mathrm{av})}$[b]	E_γ[c]
93K	93.317[a]		
		93.317±0.020	93.26±0.04
93L_I	93.317[a]		
91K	91.274		
		91.275±0.020	91.22±0.04
91L_I	91.277		
184K	184.598		
		184.595±0.040	184.46±0.27
184L_I	184.592		
209K		208.959±0.060	
300K		300.242±0.065	
393K		393.65 ±0.06	
494K		494.31 ±0.10	
		703.6 ±0.2	
		794.7 ±0.2	
888K	888.2±0.4	888.0 ±0.2	

[a] Calibration derived from $p(93L_I)/p(93K)=1.053371\pm0.000010$; K binding energy =9.659 keV; L_I binding energy =1.196 keV. 1965 adjusted values of fundamental constants used. Correction added ($\phi=4$ eV) for effective electronic work function of aluminum spectrometer chamber.
[b] Weighted average of transition energy from conversion electrons or from Ge(Li) gamma-ray spectrometry.
[c] Bent-crystal-spectrometer result of E. L. Chupp, J. W. M. DuMond, F. J. Gordon, R. C. Jopson, and H. Mark, Phys. Rev. 109, 2036 (1958).

the line position[36]; the intersection of the line median with the peak. As the upper parts of lines in our spectrometer have an axis of symmetry, this median is a substantially vertical straight line, which when extrapolated to the line peak leads to a very small uncertainty in the momentum of the intersection. For the 93-keV K line, with $\sim10^5$ counts in the top half of the line, this intercept position is conservatively located to within 2% of the FWHM, or $1:10^5$. For sources exhibiting fairly small source-degradation effects, this definition has been shown to be insensitive to these effects, as it is also to the symmetrical line broadening arising from natural linewidth. For $Z=30$, the intrinsic K-line width is ~3 eV,[37] quite negligible compared to our narrowest lines; e.g. FWHM of the 91-keV K line is ~82 eV at 0.056% resolution. Careful comparison of the best pair (statistically) of K-L_I lines, those of the 93-keV transition, gives no indication of relative K broadening.

Perhaps the small increase in the FWHM from 0.052% for the 184-keV K line to 0.056% for the 91-keV K line is due to energy degradation in the source, even at this effective thickness of 4 μg/cm^2. No evidence for the quantized, characteristic ~20-eV loss structure[40] is evident on the low sides of the line, but with a small fraction of the electrons suffering such losses this is not surprising, in comparison to the 82-eV linewidth. Obvious tailing below 10% of maximum height exists as evidence of the loss, and this becomes very severe in the K Auger-electron region, about 7 keV (see section on Auger spectrum). We consider that the line positions as defined above are not affected significantly by energy straggling.

[36] R. L. Graham, G. Murray, and J. S. Geiger, Can. J. Phys. 43, 171 (1965).
[37] Reference 32, p. 971.

Transition energies from conversion lines (Table V) were computed using the 1965 adjusted values of the fundamental constants.[38] The effect of the electronic work function of the spectrometer aluminum vacuum chamber and toroid-coil framework was corrected for by adding $\phi=4$ eV to the electron energies. For the 91-, 93-, and 184-keV transitions the assigned error is dominated by the error of the calibration constant. Note that for the 93-keV line the total error of 20 eV amounts to $\frac{1}{4}$ of the FWHM, whereas the line position is easily measurably to 2 eV (2%). The inaccuracy comes from the large (10:1) ratio of line energy to binding-energy difference. An internal standard would have markedly reduced the error.

Our values barely overlap with the larger error ranges of the crystal-diffraction-spectrometer values of Chupp *et al.*[16] for the 91-, 93-, and 184-keV transitions. (See Table V.)

The 703-, 795-, and 888-keV gamma energies were determined on the Ge(Li) spectrometer, whose calibration was based on the 93-, 184-, and 494-keV gamma energies from the electron measurements. The error of the 888-keV gamma was less than that from its K-conversion electron because of the poor statistics of the latter.

VII. K-LL AUGER SPECTRUM

Figure 9 shows the K-LL Auger spectrum of Zn as observed on the 1.5-mm-diam isotope separator deposited Ga^{67} source, with the beta-spectrometer setting which gave 0.055% FWHM at the 84-keV K-conversion line of the 93-keV transition. Comparison with this line (Fig. 2) shows the severe increase in the inelastic scattering line tails in the 7.5-keV Auger region. We attribute this degradation to the ~4 μg/cm^2 source thickness, which arises mainly from the impurity beam (probably hydrocarbon) in the isotope separator (see Sec. IIA). At the 600-eV ion deposition energy, 90% of the ions will be stopped[39] within ~1 μg/cm^2.

The scattering tails contain over 80% of the intensity of the individual lines, with the result that the tails of the intense lines in the spectrum prevented us from completely resolving the spectrum. Of the nine lines expected on the basis of intermediate electromagnetic coupling we clearly see five and resolve a sixth (K-L_3L_3, $^3P_0$) from the leading edge of the K-$L_2L_3(^1D_2)$ line.

We obtain the shape of an individual line and its scattered tail from the K-$L_2L_3(^1D_2)$ and K-$L_1L_2(^1P_1)$ lines. On these tails the structure reveals the series of quantized energy losses attributed[40] to the excitation of plasma oscillations in the solid source backing material.

[38] E. R. Cohen and J. W. M. DuMond, Rev. Mod. Phys. 37, 537 (1965).
[39] I. Bergstrom, F. Brown, J. A. Davies, J. S. Geiger, R. L. Graham, and R. Kelly, Nucl. Instr. Methods 21, 249 (1963).
[40] L. Marton, Rev. Mod. Phys. 28, 172 (1956); D. Pines, *Advances in Solid State Physics*, edited by F. Seitz and D. Turnbull (Academic Press Inc., New York, 1955), Vol. I, pp. 368–449.

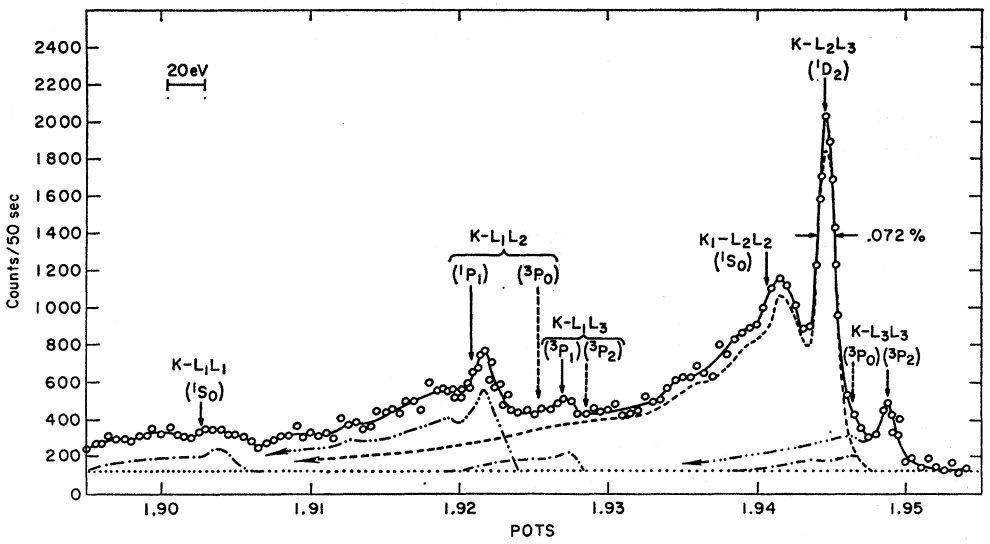

FIG. 9. K-LL Auger spectrum in Zn^{67}. Arrows indicate the calculated values of Hörnfeldt (Ref. 46), increased by 9 eV which gives approximate agreement with the K-$L_2L_3(^1D_2)$ line. Lines are resolved from the complex, guided mainly by the prominent discrete energy-loss structure of this line and the K-$L_1L_2(^1P_1)$ line.

For graphite the main energy-loss peak lies at 25 eV with a width of 6 eV, deduced[41] from optical-reflectance properties and also observed in electron scattering.[42] This agrees with the spacings of the bumps on the tail of the main (K-L_2L_3; $^1D_2$) Auger peak, and thus suggest that the main energy loss is in graphite, rather than in the ~ 4 $\mu g/cm^2$ of deposited (hydrocarbon) impurity (characteristic energy loss for collodion, the only carbon compound listed in Marton *et al.*[42] is 20 eV). Note that the width of the first loss peak, at 1.9415 "Pots," is much larger than the width (0.072%) of the main peak. If this first energy-loss peak is assigned instead as the main, undegraded peak of the K-$L_2L_2(^1S_0)$ Auger transition the minimum value for the intensity of this line (using the valley between it and the K-L_2L_3 line as background) is 0.17 of the K-$L_2L_3(^1D_2)$ peak, two to three times the expected[43,44] value. The energy of this peak is also about 6 eV higher than expected (see below). Thus considerations of width, intensity, and energy all rule out the interpretation of this bump as the K-L_2L_2-$(^1S_0)$ peak; we conclude that we cannot see it in our spectrum. Further evidence is the structure of the tail of the K-$L_1L_2(^1P_1)$ peak, which closely duplicates that of the K-$L_2L_3(^1D_2)$ tail. Similar arguments applied to the spectra of Cu($Z=29$) and Ge($Z=32$) of Sokolowski and Nordling[45] may indicate some uncertainty as to whether the K-$L_2L_2(^1S_0)$ peaks were overestimated in intensity, particularly in Cu.

One can roughly account for the increase of the observed width of the K-$L_2L_3(^1D_2)$ peak (0.072%-9 eV) over the instrumental width (0.055%-7 eV) as due to the natural K level width[37] of ~ 3 eV at $Z=30$.

Assignment of the Auger lines resolved in the spectrum is made by comparison to the table of K-LL Auger energies calculated by Hörnfeldt.[46] This computation involved a semiempirical fitting procedure, in which the energy differences between the lines in the Auger spectrum at a given atomic number are expected to be more accurate than are the absolute values. On Fig. 9 we display Hörnfeldt's values each augmented by 9 eV, which brings the K-$L_2L_3(^1D_2)$ value into approximate agreement with the peak. One sees that Hörnfeldt's energy differences progressively diverge from the experimental peaks at lower energies. The notation is that of intermediate coupling. Lines which split off from main j-j coupling peaks as "satellites" on introducing intermediate coupling are denoted by dashed lines.

Auger-line energies and intensities are given in Table VI, with Hörnfeldt's[46] energies and with intensity predictions from the graphs of collated data of Graham *et al.*,[43] and the recent theoretical predictions of Asaad[44] for comparison. Energies are corrected for the 4-eV spectrometer work function. Our energies are 7–13 eV higher than Hörnfeldt's calculations. We show in columns 6–8 of Table VI the energy discrepancies with Hörnfeldt's calculations of the measurements for $Z=29$ (Cu) and $Z=32$ (Ge) of Sokolowski and Nordling[45] together with our values. These are the best values known to us in this low-Z region. One sees a trend of disagreement appearing between Z of 32 and 30, of order 10 eV; from the approximate agreement of the differences for $Z=29$ and 30, this seems to be in the calculations. The estimated uncertainties for these calculations was given as 0.05% (3.5 eV) for $Z=30$–85.

Asaad[44] has also calculated the energy difference between the K-$L_1L_1(^1S_0)$ line and two others, the

[41] E. A. Taft and H. R. Philipp, Phys. Rev. **138**, A197 (1965).
[42] L. Marton, L. B. Leder, and H. Mendlowitz, Advan. Electron. Electron Phys. **7**, 183 (1955), Tables 16 and 17.
[43] R. L. Graham, I. Bergstrom, and F. Brown, Nucl. Phys. **39**, 107 (1962), Figs. 6 and 7.
[44] W. N. Asaad, Nucl. Phys. **66**, 494 (1965).
[45] E. Sokolowski and C. Nordling, Arkiv Fysik **14**, 557 (1958).
[46] O. Hörnfeldt, Arkiv Fysik **23**, 235 (1962).

TABLE VI. *K-LL* Auger lines.

Label[a]	Energy (eV) Observed	Calculated[b]	Intensity Observed	Predicted c	d	ΔE (Expt.-Calc.[b]) (eV) $Z=29$[e]	$Z=30$	$Z=32$[e]
K-L_3L_3 ($^3P_2$)	7566.3±1	7558	0.20 ±0.02[f]	0.17[f]	0.16[f]	6	8	−1
K-L_2L_3 ($^1D_2$)	7535.4±1	7526	1[f]	1[f]	1[f]	6	9	−1
K-L_2L_2 ($^1S_0$)	···	7493	≤0.1[f,g]	0.06[f]	0.09[f]	8		2
K-L_1L_3 ($^3P_1$)	7399±3	7392	0.046[f]±0.01	0.12[f]	0.06[f]	9	7	0
K-L_1L_2 ($^1P_1$)	7358±2	7345	0.28[f] ±0.04	0.23[f]	0.34[f]	11	13	3
K-L_1L_1 ($^1S_0$)	7220±4	7208	0.58[f]±0.02	0.07[f]	0.095[f]	15	12	−2
			"Satellites"					
K-L_3L_3 ($^3P_0$)	7550±3	7543	0.2[h] ±0.1	0.20[h]	0.22[h]		7	
K-L_1L_3 ($^3P_2$)	···	7404	≤0.5[i]	0.30[i]	0.45[i]			
K-L_1L_2 ($^3P_0$)	···	7381	≤0.12[j]	0.15[j]	0.03[j]			

[a] Designation of intermediate coupling theory (cf. Ref. 32, p. 1525).
[b] O. Hörnfeldt, Ref. 46.
[c] From Ref. 43.
[d] W. N. Asaad, Nucl. Phys. 66, 494 (1965); interpolated for $Z=30$ from Auger transition probabilities calculated with the transition amplitudes of Rubenstein and Snyder by "method A."
[e] E. Sokolowski and C. Nordling, Arkiv Fysik 14, 557 (1958).
[f] Ratio to K-L_2L_3 ($^1D_2$) line.
[g] Estimated limit from comparison of K-L_2L_3 ($^1D_2$) and K-L_1L_2 ($^1P_1$) tails.
[h] Ratio to [K-L_3L_3($^3P_2$) + K-L_3L_3 ($^3P_0$)].
[i] Ratio to [K-L_1L_3 ($^3P_1$) + K-L_1L_3 ($^3P_2$)].
[j] Ratio to [K-L_1L_2 ($^1P_1$) + K-L_1L_2 ($^3P_0$)].

K-L_3L_3($^3P_0$) and the K-L_2L_2($^1S_0$). For $Z=30$, he obtained 339 eV for the former difference. Our experimental difference is 330±5 eV, and Hörnfeldt's semiempirical prediction (see Table VI) is 335 eV.

Of the intensity predictions, only that of the K-L_1L_3-($^3P_1$) is seriously in disagreement with the value of 0.12 read from the curve[43] of Graham *et al.*; if the curve had been drawn through the experimental point at $Z=32$, the predicted value of $Z=30$ would agree with our result.

The intensity prediction of Asaad,[44] in which he takes account of configuration interaction in the final L-shell two-hole configurations $(2s)^2(2p)^4$ and $(2s)^0(2p)^6$, leads to an improved fit with measured intensities in the range $Z=23-35$. Column 6 gives these predictions based on a particular set of transition amplitudes which yield a much improved match to the trends of intensities with Z in this region. For our case, the above-mentioned discrepancy, the K-L_1L_3($^3P_1$), is rectified, but the prediction for the K-L_1L_1($^1S_0$) is in definite disagreement. Asaad indicates that this latter transition is particularly sensitive to the configuration interaction, and thus to the accuracy of the wave functions used. These were not derived by self-consistent-field methods, and as Asaad notes, the Auger calculation now requires a unified treatment over the whole range in Z with such improved wave functions.

As mentioned above, there is indication that the energy-loss tail of the dominant K-L_2L_3 peaks in $Z=29$ may have been underestimated in the spectra of Sokolowski and Nordling,[45] leading to possible overestimate of the K-L_1L_3($^3P_1$) and K-L_2L_2($^1S_0$) intensities. In fact, the experimental errors in intensities below $Z=40$ are too large to provide a sensitive test for Asaad's calculations.

In sum the Auger study reveals no significant trends, only the energy shifts indicated. A more definitive investigation will require improved, effectively thinner, sources.

ACKNOWLEDGMENTS

We wish to express our thanks to John Schiffer for suggesting the investigation of the spins of Zn^{67}, and for the communication of his experimental results before publication. We are indebted to Kent Orlandini for performing the chemical separation, to Jerome Lerner and George Lamich for operating the isotope separator, and to D. W. Engelkemeir for advice on the use of his germanium detector. Milan Oselka of the Argonne cyclotron staff arranged the sample irradiation.